Advanced classification of ionospheric troughs in midnight conditions

A.T. Karpachev

Pushkov Institute of Terrestrial Magnetism, Ionosphere, and Radiowave Propagation

(IZMIRAN), 4, Kaluzhskoe Hwy, Troitsk, Moscow, 108840, Russia,

Corresponding author:

Alexander Karpachev, e-mail: karp@izmiran.ru

Key points:

- The high latitude trough (HLT), subauroral (main) trough (MIT), and mid-latitude ring trough (RIT) were classified from the CHAMP data.

- The HLT and MIT separation is based on diffuse auroral precipitation model with two zones, equatorward and poleward.

- The MIT and RIT were separated taking into account the prehistory of all geomagnetic disturbances for the period under study.

Abstract

This study utilizes a novel technique to separate and classify different ionospheric troughs from CHAMP satellite data in the winter midnight ionosphere of the southern hemisphere at high solar activity (2000–2002). The main ionospheric trough (MIT) was separated from the high latitude trough (HLT). The separation was performed through an analysis of troughs in the frame of the model of the diffuse auroral particle precipitation. Two types of HLT were distinguished. In the mid-latitude ionosphere, the MIT was separated from the ring ionospheric trough (RIT), which is formed by the decay processes of the magnetospheric ring current. The separation was performed on the basis of an analysis of the prehistory of all geomagnetic disturbances for the period under study. In addition to the RIT, an equatorward decrease in the electron density, which is superimposed on the MIT and masks it, forms quite often at American and Atlantic longitudes.

Plain Language Summary

There are several ionization troughs in the high and mid-latitude ionosphere. The regions of their existence overlap, thus presenting a problem in trough identification. The main issues are the separation of the high latitude trough (HLT) and the main ionospheric trough (MIT), as well as that of the MIT and the ring ionospheric trough (RIT). The problem of the HLT and MIT separation was solved by carefully analyzing the positions of the troughs relative to the equatorward boundary of the diffuse auroral precipitation model and the correspondence of the MIT polar wall to the equatorward diffuse precipitation zone and that of the HLT polar wall to the poleward precipitation zone. The subauroral MIT was also separated from the mid-latitude RIT, which is formed by the decay processes of the magnetospheric ring current and exists long in the recovery phase of even a weak geomagnetic disturbance. The separation of the MIT and RIT was performed on the basis of the analysis of the prehistory of all the geomagnetic disturbances for the period under study. In addition to the MIT, a decrease in the electron density, which is superimposed on the MIT minimum and masks it, occurs at America–Atlantic longitudes.

1 Introduction

The ionization trough was discovered from the Alouette I satellite data and was described by *Muldrew* (1965) as the main ionospheric trough (MIT). Since then, many studies have explored its characteristics, which have been described in reviews (*Ahmed et al.,* 1979; *Moffett and Quegan*, 1983; *Rodger et al.,* 1992; *Karpachev*, 2003). The greatest attention has been paid to the position of the MIT minimum (see, for example, (*Kohnlein and Raitt*, 1977; *Ahmed et al.,* 1979; *Oksman*, 1982; *Karpachev et al.,* 1996; *Werner and Prolss*, 1997; *Yang et al.,* 2015; *Deminov and Shubin*, 1918; *Aa et al.,* 2010; *Karpachev et al.,* 2022). These studies reported a large data scatter, which is due to the fact that the MIT can be confused with other troughs, including high latitude troughs (HLT) and low latitude troughs (LLT) (*Werner and Prolls,* 1988; *Karpachev and Afonin*, 1989, *Karpachev*, 2019). Thus, the problem of the separation and classification of ionospheric troughs arises. Significant progress in the separation of the MIT and HLT has been made in a previous study based on CHAMP data (*Karpachev*, 2019). The MIT is a subauroral structure because it is located equatorward of the auroral oval (*Rodger et al.,* 1992). The HLT is observed inside the auroral oval (*Grebowsky et al*., 1983). With the simultaneous data on the precipitation of auroral particles, the separation of the MIT and HLT would be a routine task. However, particle precipitation on board the CHAMP has not been measured simultaneously; therefore, we were forced to use a statistical model of diffuse auroral precipitation. Thus, the current positions of troughs have been compared with some average positions of the equatorial boundary of the auroral oval (*Karpachev*, 2019). However, the current positions of the auroral oval and the troughs are often quite different from the average position. For example, the standard deviation for the MIT position is typically 2°–3°, and the data scatter is as high as ±10° (*Kohnlein and Raitt*, 1977; *Werner and Prolss*, 1997; *Aa et al.,* 2020). As a result, the highest latitude MIT case can be located inside the statistical auroral oval while the lowest latitude HLT case can be outside it.

In the present study, an advanced method is used. The key point is anthe application of a model of auroral precipitation obtained from the DMSP satellites data (*Vorobjev and Yagodkina*, 2005, 2010). This model describes the position of zone I diffuse precipitation at the equatorial edge of the auroral oval and zone II at its polar edge. As is known, the precipitation of zone I forms the polar wall of the MIT; meanwhile, the effects of zone II have never been considered. Moreover, the positions of both zones change with longitude (*Vorobjev and Yagodkina*, 2010; *Luan et al.,* 2011). Therefore, for superior efficiency, the analysis of the structures of the high latitude ionosphere was conducted herein on the basis of the framework of the longitudinal effect.

The problem of separating LLT from the subauroral MIT in the previous study was solved by removing from the CHAMP data set only the obvious cases of the so-called ring ionospheric trough (RIT) (*Karpachev*, 2019). The RIT is formed during the storm (substorm) recovery phase as a result of the decay of the magnetospheric ring current (*Karpachev*, 2021a, 2021b). However, equatorward of the MIT, in addition to the mid-latitude RIT, other electron density minima do not necessarily stand out as ionization troughs, but they significantly complicate the identification of the MIT. Therefore, this study also considered in detail the issue of the separation of the MIT and LLT.

Finally, to complete the pattern, this study highlighted the cases of a clearly expressed polar hole. In this way, the title of the paper can be interpreted broadly as the classification of electron density structures in the high and mid-latitude ionosphere. Within the framework of the advanced method, all the ionospheric troughs from the CHAMP data in the midnight winter ionosphere were thoroughly analyzed. As the main goal was to derive an accurate statement of the problem for trough separation, the analysis in the present study was limited to the southern hemisphere and high solar activity.

2 Observation data

The CHAMP satellite carried out *in situ* measurements of electron concentration *Ne* (Rother and Michaelis, 2019). Variations in *Ne* are presented below in terms of plasma frequency *fp* (Ne[cm^{-3}] = $1.24 \cdot 10^4 fp^2$[MHz]). The CHAMP altitude has changed from ~450 km to ~300 km, which is close to the height of the F2 layer maximum. It revolved on nearly polar orbit with the inclination of 87°. The CHAMP data time resolution of 15 s is less than 1° of latitude, which allows determining the minimum trough position accurately. The CHAMP data are available on the website http://op.gfz-potsdam.de/champ.

The CHAMP data for June, July, and August (i.e., for local winter conditions) in the southern hemisphere were used. The data only for high solar activity with F10.7 ~ 180 sfu for the period of 2000–2002 and the near-midnight conditions (23–01 LT) were considered. About 700 CHAMP passes in the winter high- and mid-latitude ionosphere for relatively quiet geomagnetic conditions with Kp < 4 were examined.

The MIT is usually defined by a fairly deep decrease in electron density of at least ~30%. We have not determined the level of electron density decrease in the MIT minimum. If the trough was poorly expressed on some satellite path or masked by ionospheric plasma irregularities, then the position of its minimum was determined through coordination with neighboring paths. Stricter criteria were imposed on the selection of the HLT. The HLT is observed in the auroral oval, where the electron density is highly irregular and a number of density minima can be
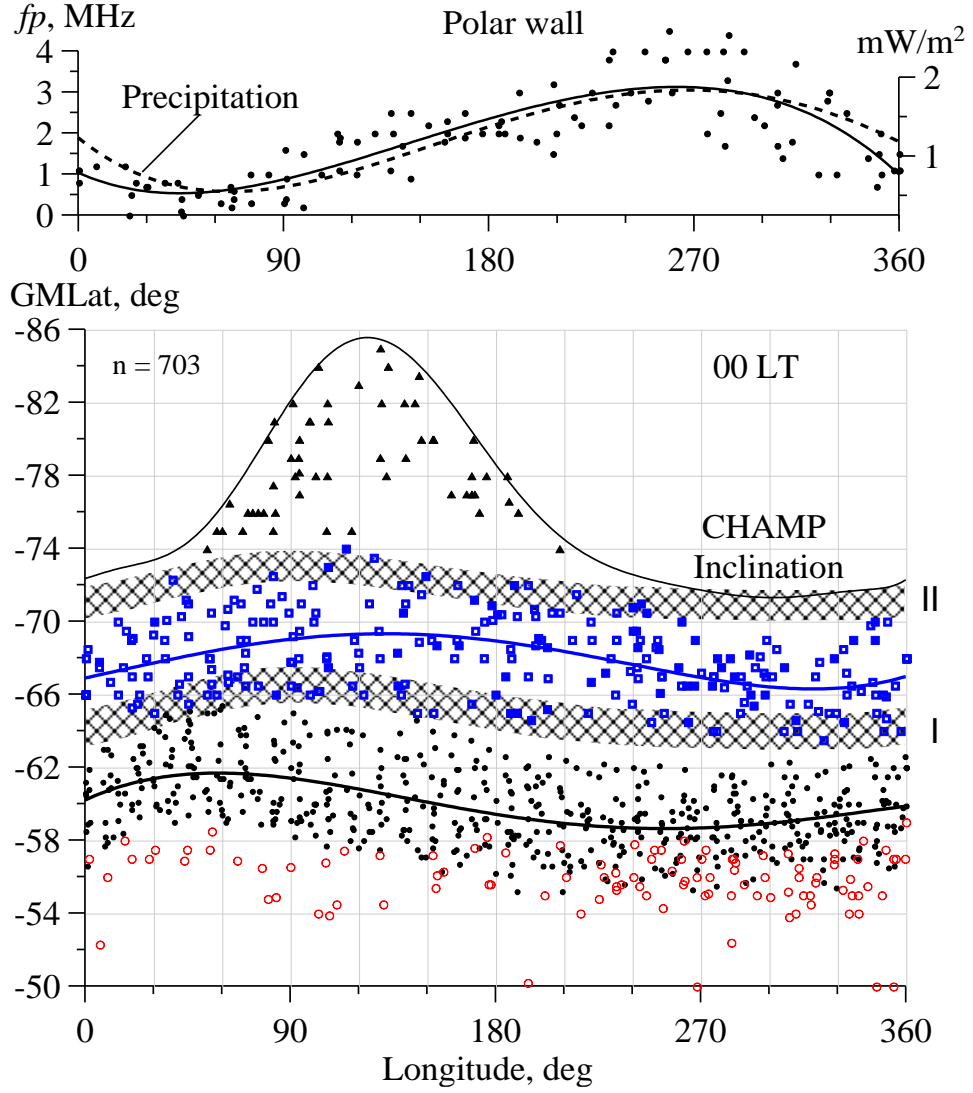
140 observed. Therefore, the HLT was recorded only in the obvious cases wherein it was clearly

141 structured and when its polar wall did not extend beyond the poleward diffuse precipitation zone.

142 Similarly, the polar hole was defined only as a broad minimum of the electron density at

143 latitudes above the poleward precipitation zone. Finally, only pronounced troughs were recorded

144 equatorward of the MIT.

145

146 **3 Structure of nighttime ionosphere**

147 An analysis of the structures of the high latitude ionosphere was conducted using a model of

148 auroral particle precipitation constructed from the DMSP satellites data in both hemispheres

149 (*Vorobjev and Yagodkina,* 2005, 2010). The model is uploaded on the website of the Polar

150 Geophysical Institute (http://apm.pgia.ru). In Figure S1 (in Supporting information), this model

151 is presented for quiet conditions. The model describes three main auroral precipitation zones:

152 diffuse auroral zone I equatorward of the auroral oval, structured auroral precipitation of the

153 auroral oval (region of auroral lights, aurora), and zone II of the soft diffuse precipitation

154 poleward of the aurora.

155 The boundaries of the precipitation zones in the near-midnight ionosphere change with

156 longitude (*Vorobjev and Yagodkina*, 2010; *Luan et al.,* 2011), as well as the position of the MIT

157 (*Karpachev et al.*, 2018). For the southern hemisphere, these boundaries are presented in Figure

158 S2 (in Supporting information) according to (*Luan et al.,* 2011). The equatorward and poleward

159 boundaries of the oval experience synchronous longitudinal variations with an amplitude of

160 ~2.5°. Therefore, it is most effective to analyze the structures of the high latitude ionosphere in

161 terms of geomagnetic latitude–geographic longitude. Figure 1 shows the positions of the

162 different structures in the winter midnight (23–01 LT) ionosphere of the southern hemisphere.

163 To eliminate the dependence on geomagnetic activity, the positions of the MIT, RIT, and HLT

164 were reduced to Kp = 2 according to $\Lambda corr = \Lambda c - a(Kp(\tau) - 2)$, where Λc is the current position

165 of the structure and the ***a*** factor is 2.0 for the MIT according to (*Karpachev et al.,* 1996), 1.5 for

166 the RIT according to (*Karpachev,* 2021b), and ~1.5 for the HLT according to (*Grebowsky et al*.,

167 1983). The Kp(τ) index was used as it considers the prehistory of geomagnetic activity

168 development (*Deminov and Shubin*, 2018). In Figure 1, zones I and II of the diffuse precipitation

169 taken from Figure S1 are shaded. The average (for all longitudes) position of the equatorial

170 boundary of the auroral precipitation oval corresponds to 64° at Kp = 2 (*Karpachev*, 2019). The

171 upper curve in Figure 1 corresponds to the CHAMP satellite inclination. The satellite inclination

172 of 87° does not limit the observations of the discussed structures, except for the polar hole. But

173 polar hole cases are shown in Figure 1 solely for the completeness of the pattern; only

174 unambiguous cases were selected.

175

Figure 1. On the top: Longitudinal variations in the magnitude of MIT polar wall (dots and approximation) and averaged auroral precipitation energy flux at 21–03 MLT under Kp = 2 (dashed line) [*Luan et al.,* 2011]. On the bottom: Longitudinal variations in the positions of main structures in the near-midnight winter ionosphere of the southern hemisphere: polar hole (triangles), HLT1 (empty squares), HLT2 (filled squares), MIT (dots), RIT, and electron density minima (red circles). The shaded latitude belts show the diffuse auroral precipitation of zones I and II. The upper curve represents the CHAMP inclination equal to 87°.

The black dots in Figure 1 depict the cases of MIT observations (n = 703). The approximating curve demonstrates the longitudinal effect in the MIT position with an amplitude of ~3° and a correlation coefficient of 0.52. The scatter of the data (standard deviation) is 1.85°, which is less than the 2°–3° range that is usually observed in the statistical processing of trough data. In the first approximation, the variations in the MIT position are consistent with the

191   variations in the position of the precipitation of zone I. The MIT was separated from the HLT
192   (blue squares) at the high latitude boundary of the MIT occurrence region. Figure 2a shows the
193   simplest case when both troughs are observed simultaneously. This case allows us to draw a
194   fundamentally important conclusion: the MIT polar wall is, as usual, determined by the
195   precipitation of zone I, and the HLT polar wall is undoubtedly formed by the precipitation of
196   zone II. The latter fact is the key to the identification of the HLT type I. The HLT was previously
197   studied in detail from *Ni* variations recorded on board OGO-6 at heights of 400–1,100 km
198   (*Grebowsky et al.,* 1983) and from EISCAT radar data (*Williams et al.*, 1986). In particular, the
199   statistical position of HLT relative to the auroral oval was determined (*Grebowsky et al.,* 1983).
200   The authors observed the HLT exclusively within the auroral oval and attributed its formation
201   ultimately to the action of electric fields in the zone of the high latitude ionospheric plasma
202   convection. These fields cause the frictional heating of the plasma and its outflow upward; both
203   cases lead to an increase in recombination and, consequently, to the formation of the trough.
204   Since this effect is observed in a limited region, the HLT of this type is usually narrow (3°–5° in
205   latitude). Such a trough is observed in Figure 2b together with the polar hole. We define such a
206   trough as HLT2; it is depicted with crosses in Figure 1. Figure 2c shows a rather rare example of
207   the simultaneous observation of the three troughs: MIT, HLT2, and HLT1. Figure 1 shows that
208   HLT2 is observed less frequently than HLT1. In Figure 2, an approximation curve for all HLTs
209   is drawn.

210   In the eastern hemisphere, at longitudes of 30°–90°E, the MIT is located at the highest
211   latitudes so that the region of its existence overlaps with the precipitation of zone I and the
212   region of HLT existence. In the region of the intersection of the two sets of troughs, the problem
213   of separation becomes particularly acute. Therefore, all cases of trough observations in this
214   region were analyzed thoroughly. The main result of this analysis was rather unexpected.
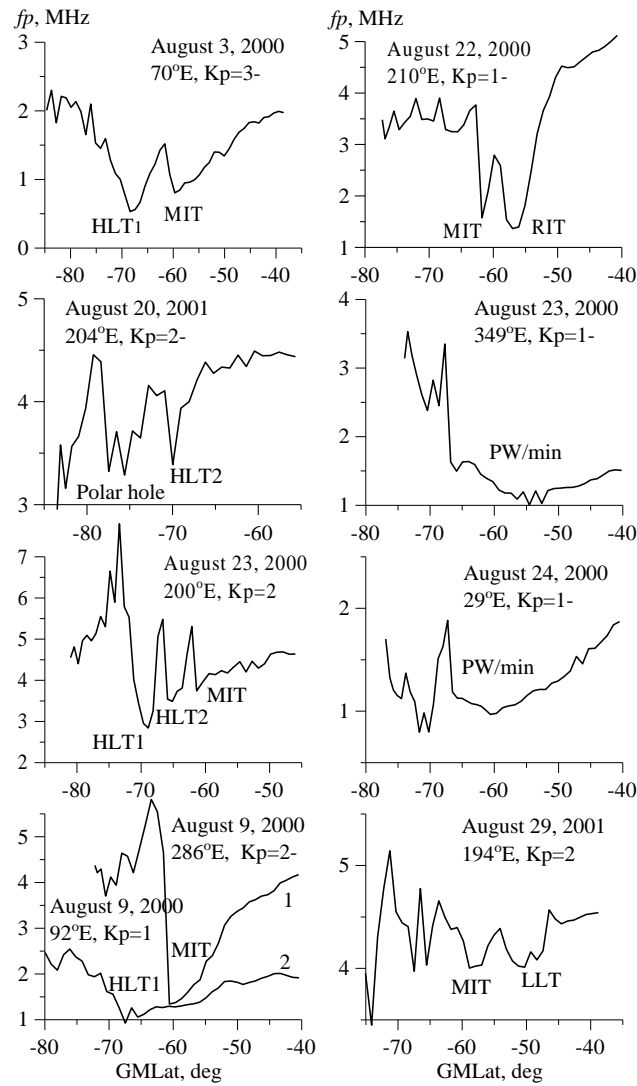
215

Figure 2. The most characteristic examples of troughs in the nighttime winter ionosphere of the southern hemisphere. Local time changes from 23.8 to 0.9 h. Details are in the text.

The top panel in Figure 1 shows the variations in the magnitude of the polar wall derived from the CHAMP data for the quiet period of August 15–24, 2000 (dots and approximation line). The dashed line depicts the longitudinal variations in the average electron flux calculated at latitude of −65° GMLat from the colored Figure 2S from (*Luan et al.,* 2011). As expected, the magnitude of the polar wall is completely determined by the precipitation. Electron precipitation is much stronger in the western hemisphere than in the eastern hemisphere. Therefore, in the western hemisphere, the precipitation forms a pronounced polar wall of the MIT, and it is always clearly determined. This illustrates the latitudinal *fp* cross-section 1 in Figure 2d, which represents the MIT recorded on August 9, 2000, at longitude of 286°E at 0.6 LT and Kp = 2-. Different scenarios can be realized in the eastern hemisphere. If the precipitation of zones I and II is still quite intense, they form (weak) peaks of electron density, and both troughs are

232 observed. If the precipitation in one of the zones is very weak, then either the MIT or the HLT

233 can be formed. For example, curve 2 in Figure 2d represents the latitudinal *fp* cross-section

234 obtained on August 7, 2000, at longitude of 100°E at 0.5 LT and Kp = 1+. There is no peak of

235 electron density; only the relative minimum of *Ne* at the MIT latitudes. Therefore, the MIT is not

236 identified. The minimum of the electron density is observed much poleward at latitude of −68°,

237 and it certainly belongs to HLT1 because its polar wall is formed by the precipitation of zone II.

238 Note that this trough can be easily confused with the MIT in a cursory analysis. Finally, if both

239 zones have no precipitation, then a monotonous decrease is recorded in the electron density to

240 the pole without peaks and troughs. Such cases correspond to the value *fp* close to 0 in Figure 3.

241 The red circles in Figure 1 depict the troughs and quasi-troughs that were observed

242 equatorward of the MIT. The main one among them is the RIT. It is formed during the recovery

243 phase of a geomagnetic storm and even a weak substorm as a result of the decay of the

244 magnetospheric ring current. The dynamics of this mid-latitude trough is described in detail in

245 (*Karpachev*, 2021a, 2021b). When the MIT and RIT are simultaneously observed, their

246 identification is not difficult; the equatorward trough is the RIT (Figure 2e). However, during a

247 storm, any situation can be observed: both troughs, one MIT or one RIT. Moreover, the MIT can

248 be identified on one path, and the RIT on the next path. Therefore, the main method of MIT and

249 RIT separation is an analysis of the prehistory of the development of geomagnetic disturbance

250 (*Karpachev*, 2021a, 2021b). Herein, even weak geomagnetic disturbances for the period under

251 consideration were analyzed to separate the RIT from the MIT. An example of such an analysis

252 is applied below in the discussion of Figure 3.

253 Figures 2f,g,h show examples of structures that can be defined as quasi-troughs. Figure 2f

254 shows the latitudinal *fp* cross-section typical for the longitudes of America and the Atlantic. A

255 steep polar wall of the trough, a shallow minimum of the electron density slightly equatorward

256 (at −65.5°), and a deep and wide minimum at −55° are observed in Figure 2f. How is the position

257 of the MIT determined in this case? The latitude of −65.5° for Kp = 1- corresponds rather to the

258 polar wall of the MIT, and the latitude of −55° completely goes beyond the existence region of a

259 "normal" MIT. Similarly, the position of the *Ne* minimum at latitude of −60.5° for Kp = 1- in

260 Figure 2g is definitely lower than the "normal" position of the MIT at longitude of 29°E (Figure

261 1). The well-defined polar wall of the trough helps to solve this problem. In the near-midnight

262 hours, the base of the polar wall usually coincides with the equatorial boundary of diffuse

263 precipitation (*Rodger et al.,* 1986). The MIT minimum is located within 5° equatorward of this

264 boundary (*Rodger et al.,* 1992), and the minimum distance is about 2° (*Slater et al*., 1980);

265 therefore, the MIT minimum is usually 3°–4° equatorward of the polar wall. If the minimum of

266 the MIT 3°–4° equatorward of the polar wall is determined in Figures 3f and 3g, then in both

267 cases, the trough minimum will correspond to an average MIT position. As for the reason for the

268 formation of an additional minimum of electron density, we should note that the geomagnetic

269 latitude of −56° at longitude of 285° approximately corresponds to the geographical latitude of

270 −66°, that is, the Arctic Circle. The Arctic Circle limits the area of the polar night in winter

271 conditions, wherein there is no solar ionization and the electron density decays. The influence of

272 the polar night affects a fairly wide range of longitudes from 120°W to 30°E.

273 Finally, Figure 2h shows an example of a clearly defined minimum of electron density

274 recorded on August 29, 2001, at latitude of −50.2° and longitude 194°E. Several more well-

275 expressed LLTs were observed at latitudes 50° and equatorward (not shown in Figure 1). They

276 apparently belong to the class of LLTs discovered in (*Karpachev*, 2021c).

277

278 **4 Events on August 19 and 21, 2000**

279 Trough identification is obviously a challenge. In some cases, data analysis turns into a

280 complicated investigation. Figure 3 shows two examples that required such an investigation.

281 Figure 3 on the left shows the longitudinal variations of ionospheric structures for August 19

282 (top) and August 21 (bottom), 2000. The data were obtained in the near-midnight sector for the

283 average value of Kp = 1 on August 19 and Kp = 2+ on August 21. However, at the beginning of

284 August 21, the Kp index increased from a value of 1 to 3+, and this change was enough to form a

285 deep RIT (red circles in Figure 3), which was then observed all day in a pronounced form. The

286 examples are observed on paths 7, 15, and 25 in Figure 3 on the right. The MIT identification

287 was a challenge. Its position was clearly defined only on paths 3 and 15. Conversely, the HLT

288 was clearly revealed all day, as shown by the paths 3, 7, 15, and 25 on the right of Figure 3. In

289 very quiet conditions on August 19, RIT did not manifest itself. On paths 2, 4, and 6, the MIT

290 was clearly expressed, and its position could be determined either by the base of the polar wall

291 (PW) or by the *fp* minimum (red circles), which formed clearly below the model position, as

292 discussed previously. The rest of the time, the MIT manifested itself at best in the form of a

293 small minimum of electron density, as observed on paths 14 and 24. HLT was also clearly

294 manifested, particularly on paths 4, 14, and 24. On path 8, only HLT was observed. Therefore, in

295 both cases, there was a well-expressed HLT, and on August 21, RIT was also well-expressed.

296 Much effort was needed to distinguish the MIT in both cases. Moreover, on path 8 on August 19

297 under manual and automatic data processing, the HLT would have been identified as the MIT.

298 Hence, we are skeptical about the automatic processing of data on the trough.
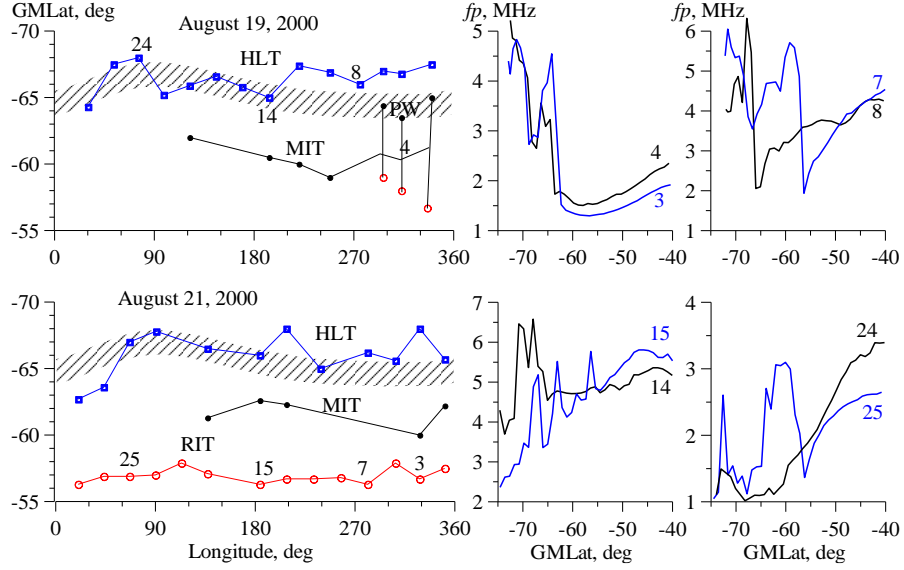
299

300

Figure 3. On the left: Longitudinal variations in the position of HLT (blue squares) and MIT (black circles) on August 19 (top) and August 21 (bottom), 2000. Red circles show the positions of the *fp* minima (top) and RIT (bottom). The shaded latitude belts show the diffuse auroral precipitation of zones I and II. On the right are the latitudinal profiles of *fp* for the paths marked in the Figure on the left.

5 Conclusion

Undoubtedly, considerable progress has been made in the separation and classification of the various structures of the nighttime high latitude and mid-latitude ionosphere. The success is based on several factors. First, the CHAMP large data set allows the consideration of a phenomenon from different angles. Second, all complex cases were analyzed carefully, and automatic data processing was found to be questionable. Third, the problem could only be solved after many years of experience. Note that the solution to the problem could be traced back to 1998 (*Karpachev*, 1998), and it was continued in 2019 (*Karpachev*, 2019). Fourth, the idea of separating MIT, HLT1, and HLT2 arose from a simple and illustrative model of diffuse auroral precipitation (*Vorobjev and Yagodkina*, 2005). It describes precipitation zone I on the equatorial edge of the auroral oval and zone II on its polar edge. It turned out that precipitation of zone 2 forms the PW of HLT1, similar to the way the precipitation of zone I forms the PW of the MIT. This point is key in the separation of MIT and HLT1.

As the boundaries of both zones change with longitude by 2.5° (*Luan et al.,* 2011), similar to the longitudinal variations in the MIT position, the analysis is most effective when performed in the framework of the longitudinal effect. The problem of the separation of MIT and HLT1 was

found to be radically different in the western and eastern hemispheres. In the western hemisphere, the MIT is located at lower latitudes than in the eastern hemisphere and is equatorward of the auroral oval. In the western hemisphere, the intensive precipitation forms a very steep and high PW of the MIT. These conditions facilitate the separation of MIT and HLT. In the eastern hemisphere, MIT shifts to high latitudes so that the region of its existence at longitudes 30°–90°E overlaps with zone I of the precipitation and the region of HLT existence. In addition, the weak precipitation at longitudes of 0°–90°E produces much less expressed and irregular electron density structures. Therefore, at these longitudes, each case was considered especially carefully, and the separation of MIT and HLT1 was carried out according to the correspondence of the PW to the precipitation of zone I or II. The pattern is complicated by the presence of a second high latitude trough (HLT2) described in (*Grebowsky et al.,* 1983; *Williams et al.*, 1986). Fortunately, HLT2 differs in that it is relatively narrow in latitude (3°–4°).

The mid-latitude troughs (and sub-troughs) located equatorward of the MIT were also clearly separated from the MIT for the first time. The main one among them is the RIT. It is formed even after a weak enhancement of geomagnetic activity, and it can be observed for a long time (sometimes for two days) at latitudes near L ~ 3 (*Karpachev*, 2021a, 2021b). It is no less difficult to separate the MIT from the RIT than the MIT from the HLT, but the methodology for such a separation has been carefully developed earlier (*Karpachev*, 2021a, 2021b). It is based mainly on the prehistory of the disturbance development. Therefore, even the weak geomagnetic disturbances during the period under consideration were carefully analyzed. Note that RITs are more often formed at longitudes with a weak geomagnetic field, i.e., in the western hemisphere.

The quasi-trough is understood as an additional minimum of the electron density equatorward of the MIT, and it is often observed at the longitudes of America and Atlantic. It is assumed to be related to the decay of the electron density beyond the polar circle during the polar night. This minimum deepens the MIT and therefore prevents the determination of the exact position of the MIT. Finally, several troughs too far from the mean MIT position (<50°) were recorded, and they, apparently, belong to LLTs (*Karpachev*, 2021c).

The result of this analysis is a more accurate determination of the MIT position: the standard deviation of 1.85° is less than that in other statistical studies, and the scatter has decreased to ±4°. This allows to significantly refine the model of the MIT position.

The study considers the structure of the ionosphere for limited conditions: high solar activity, winter, southern hemisphere, and near-midnight conditions. Preliminary analysis shows that the structure of evening and morning ionosphere is quite different from the considered structure. The same is particularly true for the daytime ionosphere. Consequently, this work should be

360 considered as a statement of the problem, which implies the need for further research. The
361 analysis of the structure of the evening and morning ionosphere is prepared for publication.
362
363

370
371

372   **References**
373 Aa, E., Zou, S., Erickson, P., Zhang, S-R., and Liu, S. (2020), Statistical analysis of the main
374   ionospheric trough using Swarm in situ measurements, *J. Geophys. Res., 125*,
375   e2019JA027583. doi.org/10.1029/2019JA027583.
376 Ahmed, M., Sagalyn, R.C., Wildman, P.J.L., and Burke, W.J. (1979), Topside ionospheric
377   trough morphology: occurrence frequency and diurnal, seasonal and altitude variations. *J.*
378   *Geophys. Res., 84*(2), 489–498. doi.org/10.1029/JA084iA02p00489.
379 Deminov, M.G., and Shubin, V.N. (2018), Empirical model of the location of the main
380   ionospheric trough, *Geomagnetism and Aeronomy, 36*(4), 45–52.
381   doi.org/10.1134/S0016793218030064.
382 Grebowsky, J.M., Tailor, H.A., and Lindsay, J.M. (1983), Location and source of ionospheric
383   high latitude troughs, *Planet. Space Sci., 31*(1), 99–105. doi.org/10.1016/0032-
384   0633(83)90034-X.
385 Karpachev, A.T., Deminov, M.G., and Afonin, V.V. (1996), Model of the mid-latitude
386   ionospheric trough on the base of Cosmos-900 and Intercosmos-19 satellites data. *Adv.*
387   *Space Res., 18*(6). 221–230. doi.org/10.1016/0273-1177(95)00928-0.
388 Karpachev, A.T. (2003), Dependence of the MIT shape on longitude, altitude, season, local time,
389   solar and magnetic activity, *Geomagnetism and Aeronomy, 43*(2), 256–269.
390 Karpachev, A.T., Klimenko, M.V., and Klimenko, V.V. (2018), Longitudinal variations of the
391   ionospheric trough position, *Adv. Space Res.,* doi.org/ 10.1016/j.asr.2018.09.038.
392 Karpachev, A.T. (2019), Variations in the winter troughs' position with local time, longitude,
393   and solar activity in the Northern and Southern hemispheres. *J. Geophys. Res., 124*(10).
394   8039–8055. doi.org/10.1029/2019JA026631.

395 Karpachev, A.T. (2021a), Dynamics of main and ring ionospheric troughs at the recovery phase
396   of storms/substorms. *J. Geophys. Res., 126*, e2020JA028079.
397   doi.org/10.1029/2020JA028079.

398 Karpachev, A.T. (2021b), Statistical analysis of ring ionospheric trough characteristics. *J.*
399   *Geophys. Res., 126*(10), e2021JA029613. doi:10.1029/2021JA029613.

400 Karpachev, A.T. (2021c). Sub-auroral, mid-latitude, and low-latitude troughs during severe
401   geomagnetic storms. *Remote Sensing.*, *13*(3), 534; doi.org/10.3390/rs13030534.

402 Karpachev, A.T., Klimenko, M.V., Klimenko, V.V., Chirik, N.V., Zhbankov, G.A., and
403   Pustovalova, L.V. (2022), Satellite model of foF2 in winter high-latitude ionosphere
404   describing the trough structure. *Adv. Space Res.*, 69(1), 2-15. doi:10.1016/j.asr.2021.07.014.

405 Kohnlein, W., and Raitt, W.J. (1977), Position of the mid-latitude trough in the topside
406   ionosphere as deduced from ESRO-4 observations. *Planet. Space Sci., 25*(5/6), 600–602.
407   doi.org/10.1016/0032-0633(77)90069-1.

408 Luan, X., Wang, W., Burns, A., Solomon, S., Zhang, Y. Paxton, L. J. and Xu, J. (2011),
409   Longitudinal variations of nighttime electron auroral precipitation in both the Northern and
410   Southern hemispheres from the TIMED global ultraviolet imager. *J. Geophys. Res., 116*,
411   A03302, doi:10.1029/2010JA016051.

412 Moffett, R.J., and Quegan S. (1983), The mid-latitude trough in the electron concentration of the
413   ionospheric F-layer: A review of observations and modeling. *J. Atmos. Terr. Phys., 45*(5),
414   315–343. doi.org/10.1016/S0021-9169(83)80038-5.

415 Muldrew, D.B. (1965), F layer ionization troughs deduced from Alouette data. *J. Geophys. Res.,*
416   *70*(11), 2635–2650. doi.org/10.1029/JZ070i011p02635.

417 Oksman, J. (1982). Apparent diurnal movements of the trough in total electron content (TEC) of
418   the ionosphere. *Geophysica, 19*(1), 13–22.

419 Rodger, A.S., Brace, L.H., Hoegy, W.R., and Winningham, J.D. (1986), The poleward edge of
420   the mid-latitude trough – its formation, orientation and dynamics. *J. Atmos. Terr.*
421   *Phys.,48*(8), 715–728. doi.org/10.1016/0021-9169(86)90021-8.

422 Rodger, A.S., Moffett, R.J. and Quegan, S. (1992), The role of ion drift in the formation of
423   ionisation troughs in the mid-and high-latitude ionosphere – a review. *J. Atmos. Terr. Phys.,*
424   *54*(1), 1–30. doi.org/10.1016/0021-9169(92)90082-V.

425 Rother, M., Michaelis, I. (2019). CH-ME-2-PLPT - CHAMP Electron Density and Temperature
426   Time Series in Low Time Resolution (Level 2). GFZ Data Services.

427 Slater, D.W., Smith, L.L., and Kleckner, E.E. (1980), Correlated observations of the equatorward
428   diffuse auroral boundary. *J. Geophys. Res., 85(2)*, 531–542.
429   doi.org/10.1029/ja085ia02p00531.

430 Vorobjev, V.G. and Yagodkina, O.I. (2005), Effect of magnetic activity on the global
431   distribution of auroral precipitation zones. *Geomagnetism and Aeronomy*, 45(4), 467–473.
432 Vorobjev, V.G., and Yagodkina, O.I. (2010), Seasonal and diurnal (UT) variation in the
433   boundaries of the auroral precipitation and polar cup. *Geomagnetism and Aeronomy, 50*(5),
434   625–633. doi.org/10.1134/S0016793210050063.
435 Werner, S., and Prolss, G.W. (1997), The position of the ionospheric trough as a function of
436   local time and magnetic activity. *Adv. Space Res., 20*(9), 1717–1722. doi.org/10.1016/S0273-
437   1177(97)00578-4.
438 Williams, P.J.S., and Jain, A.R. (1986), Observations of the high latitude trough using EISCAT.
439   *J. Atmos. Terr. Phys., 48*(5), 423–434. doi.org/10.1016/0021-9169(86)90119-4.
440 Yang, N., Le, H. and Liu, L. (2015), Statistical analysis of ionospheric mid-latitude trough over
441   the Northern hemisphere derived from GPS total electron content data. *Earth, Planets and
442   Space*, *67*, 196. doi.org/10.1186/s40623-015-0365-1.
443